Journal of Thermal Engineering

CONFERENCE ON ADVANCES IN MECHANICAL ENGINEERING ISTANBUL 2016 – ICAME2016
11-13 May 2016, Yildiz Technical University, Istanbul, Turkey

2-D NUMERICAL INVESTIGATION ON THE EFFECTS OF BLADE NUMBER ON THE CENTRIFUGAL BLOWER

*** MEHMET SALİH CELLEK**
Heat and Thermodynamics Division, Department of Mechanical Engineering, Mechanical Engineering Faculty, Yildiz Technical University, Yildiz, Besiktas, Istanbul 34349, Turkey

TAHSİN ENGİN
Department of Mechanical Engineering, Applied Fluid Mechanics Laboratory, Faculty of Engineering, Sakarya University, Sakarya 54187, Turkey

ALİ PINARBAŞI
Heat and Thermodynamics Division, Department of Mechanical Engineering, Mechanical Engineering Faculty, Yildiz Technical University, Yildiz, Besiktas, Istanbul 34349, Turkey

Keywords: Blade number, forward-curved blade, blower
** Corresponding author: Phone:+900212 383 28 22*
E-mail address: mscellek@yildiz.edu.tr

ABSTRACT

Energy conversion applications are directly affected through the employment of turbomachines and their efficiencies. Therefore, it is crucial to focus on their components namely impellers and volute casing. The blade number, being one of the impeller parameter, effects the turbomachine's overall performance. Therefore parametric investigation is requirement for the best selection.

The purpose of this paper is to investigation the effects of blade number on the performance of a centrifugal blower by means of Computational Fluid Dynamics (CFD). The results obtained in this study show that the blade number is one of the important parameter to effect of the performance characteristics of the centrifugal blower. With the increment in the blade number of the impeller, the shaft power, total pressure and velocity at the outlet increase. However the hydraulic efficiency decrease. The results clear that a significant attention must be given to impeller selection.

The three-dimensional, incompressible Navier-Stokes equations over the unstructured mesh are accomplished with commercial software ANSYS Fluent.

INTRODUCTION

Turbomachines such as pumps, fans, turbines and compressors are extensively used in the industry. Specific turbomachines are utilized for energy production purposes such as steam and water turbines, while other types including fans, compressors and pumps consume energy to increase the fluid pressure. Due to their common use and the importance of the energy, specific consideration is requirement for selecting the convenient components for operating [1].

Blowers are one of the most common used industrial devices for transfer the air or other gas from one point to another. They have relatively high pressure ratio (up to 1.2) than fans (up to 1.1). In additional they deliver high volume flow rate. A centrifugal blower unit typically utilized in automotive climate control systems [2]. On the other hands, fans are extensively used in heating, ventilation, air conditioning systems and numerous other applications. But the lower efficiency and higher noise level of centrifugal fans than those of axial fans are the primary deficiencies of these machines [3].

Recent developments in the Computational Fluid Dynamics (CFD) lead to specific important facilities to

design turbomachines with the complex and the high turbulence internal flows. Thus, it allows interpreting the design procedure and optimizing the product components without the high cost and less waste of time before the manufacturing process. Besides, it enables us to study the effects of various parameters on these components [1].

Zhou et al. [4] investigated the performance of centrifugal pumps with three different impeller (one has four straight blade and the other two have six twisted blades) with the commercial CFX with the use of the standard k-ε turbulence model. It was concluded from the study that the predicted results relating to the twisted-blade impeller were better than those relating to the straight blade impeller. Madhwesh et al. [5] investigated the impact of the splitter blade at different locations on the impeller of a centrifugal fan. The results exhibited that the splitter blade provided at the impeller leading edge provides pressure recovery of the fan outlet. However, there is not a significant static pressure recovery at the trailing edge near the suction side and the circumferential mid-span of the splitter blades. When the splitter blades located at the trailing edge near the pressure side of the main blades, the static pressure almost decreases.

Lee and Lim [6] studied numerically and experimentally various fan ribs in the centrifugal blower based on performance assessments. The results showed that the flow rate gradually increased to a value 7% higher than the existing model based on the exit shape of the fan. In additional, the forward-curved fan ribs showed the best the best performance among the studied four different impellers.

In the study of Baloni et al. [7], the flow fields inside a centrifugal blower were investigated at various angular, radial and axial locations in the volutes based on the two design principle of constant angular momentum and constant mean velocity. The experiments were conducted with full throttle open condition at inlet with the using three-dimensional probe. The results show that the flow within the volute casing based on the constant velocity design concept present better flow condition.

Datong et al. [8] studied experimentally the noise characteristics of the forward curved blades centrifugal fan. To investigate the effects of inclined volute tongue, impeller blade-tongue clearance, hub-volute clearance and their coupling effect to the performance and noise of the forward curved blades, some different volute geometric configurations tested. The results showed that a good coupling modification not only reduces the fan tonal noise but also advances the fan performance also extends the operating range.

In this study, the performance of the centrifugal blower with the 30, 40 and 50 forward curved blades are investigated. The effects of the blade number on the flow pattern visualized with the Ansys Post Processing Tool.

NUMERICAL MODELLING

Centrifugal blower geometry and mesh generation

The schematic of the centrifugal blower is shown in Figure 1. The main blower consists of 30 blades, each with a chord length of 13.5 mm. To investigate the effects of blade number, two impellers are created with 40 and 50 blades. The blades are located approximately 56.5 mm (measured from the leading edge) from the center of rotation. The radius of the outer wall varies logarithmically from 80 mm to 146.5 mm. The total pressure at the inlet is defined to be 200 Pa and the flow discharges to ambient conditions (static pressure = 0 Pa). The blades are rotating with an angular velocity of 261 rad/s. The flow is assumed to be turbulent [2].

In the study, unstructured mesh was utilized for the simulation. In order to mesh independence, approximately 9000, 12500 and 36000 mesh numbers were studied and finally 36000 elements was selected for the simulations.

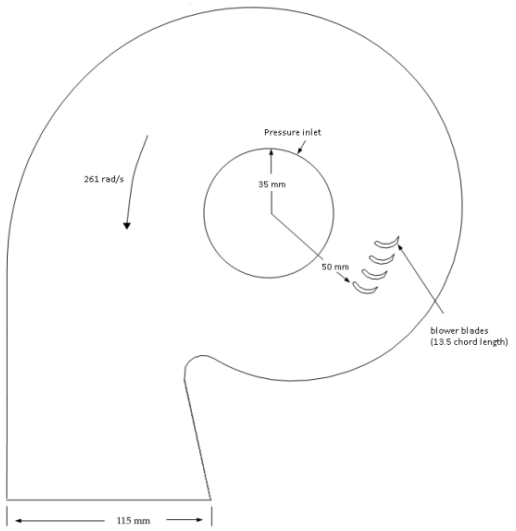


Figure 1. Schematic view of the centrifugal blower

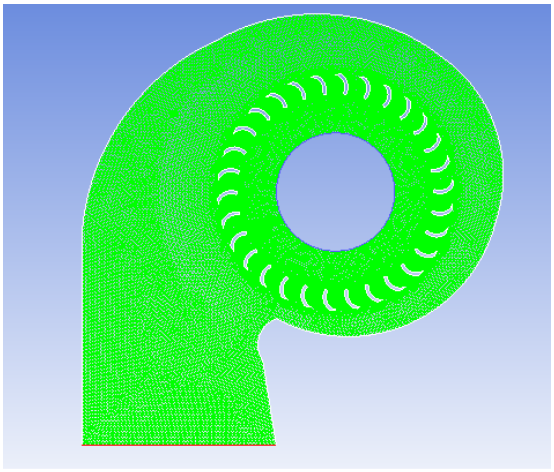


Figure 2. Generated mesh of the centrifugal blower

Governing equations and boundary conditions

In this study, the Reynolds-averaged Navier-Stokes equation was calculated by means of commercial software package Fluent that helps in achieving a finite volume approach for the solutions [9]. The steady and three dimensional incompressible flow through the rotating impeller solved in a moving reference with constant rotational speed. Moreover the flow through the stationary parts of the pump is solved in an inertial reference frame. The governing equations for the rotating impeller and stationary parts of the pumps are formulated as follows, neglecting the energy equation and the gravity [10]:

$$\nabla \rho \mathbf{u_r} = 0 \tag{1}$$

$$\nabla \rho \mathbf{u_r} = 2\rho\omega \times \mathbf{u_r} + \rho\omega \times \omega \times r = -\nabla p + \mu_{eff}\nabla^2 \mathbf{u_r} \tag{2}$$

$$\nabla \rho \mathbf{u} = -\nabla p + \mu_{eff}\nabla^2 \mathbf{u} \tag{3}$$

where $\mathbf{u_r}$ is the velocity vector in a rotating system, on the other hand $\mathbf{u}$ is the local vector in the stationary frame of reference, $\boldsymbol{\omega}$ is the rotational speed, p is the pressure, μ_{eff} is the dynamic effective viscosity which is a linear combination of laminar and turbulent viscosity derived from $k-\varepsilon$ model of turbulence. Standard $k-\varepsilon$ turbulence model, which has been widely utilized for the prediction of turbulence, is selected because of the capability and satisfactory results in the turbomachinary [11, 12].

The turbulence kinetic energy (k) and turbulence dissipation rate (ε) can be presented with the differential transport equations as follows [10]

$$\nabla \rho \mathbf{u} k = \nabla\left(\left(\mu + \frac{\mu_t}{\sigma_k}\right)\nabla k\right) + G_k - \rho\varepsilon \tag{4}$$

$$\nabla \rho \mathbf{u} \varepsilon = \nabla\left(\left(\mu + \frac{\mu_t}{\sigma_\varepsilon}\right)\nabla \varepsilon\right) + C_{1\varepsilon}\frac{\varepsilon}{k}G_k - C_{2\varepsilon}\rho\frac{\varepsilon^2}{k} \tag{5}$$

$$\mu_t = \rho C_\mu \frac{k^2}{\varepsilon} \tag{6}$$

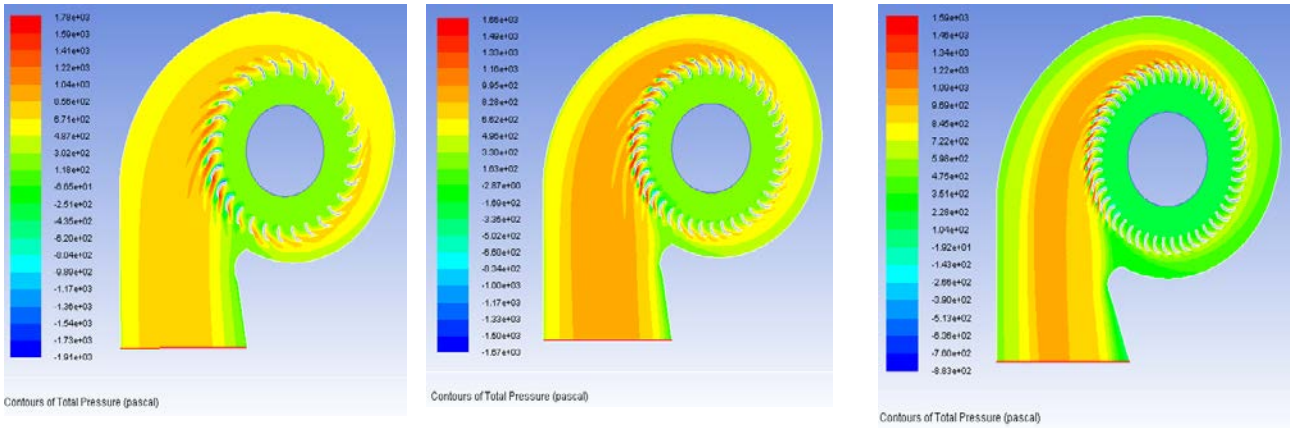
where $\mathbf{u}$ stands for velocity component in the corresponding direction, σ_k and σ_ε are the turbulent Prandtl numbers for k and ε. μ is the laminar viscosity, μ_t represents the turbulence viscosity, G_k represents the generation of turbulent kinetic energy due to the mean velocity gradients. Adjustable constants used in the equations are below [10].

$$C_\mu = 0.09,\ C_{1\varepsilon} = 1.44,\ C_{2\varepsilon} = 1.92,\ \sigma_k = 1.0, \sigma_\varepsilon = 1.3$$

The standard wall functions were used for near the wall treatment [10]. The turbulence intensity and the hydraulic diameter involved parameters are estimated with values of 5% and D, respectively. The numerical algorithm is utilized SIMPLE, in which the pressure parameter is discretized using the second-order upwind scheme [13,14]. The second order upwind scheme is used for spatial discretization.

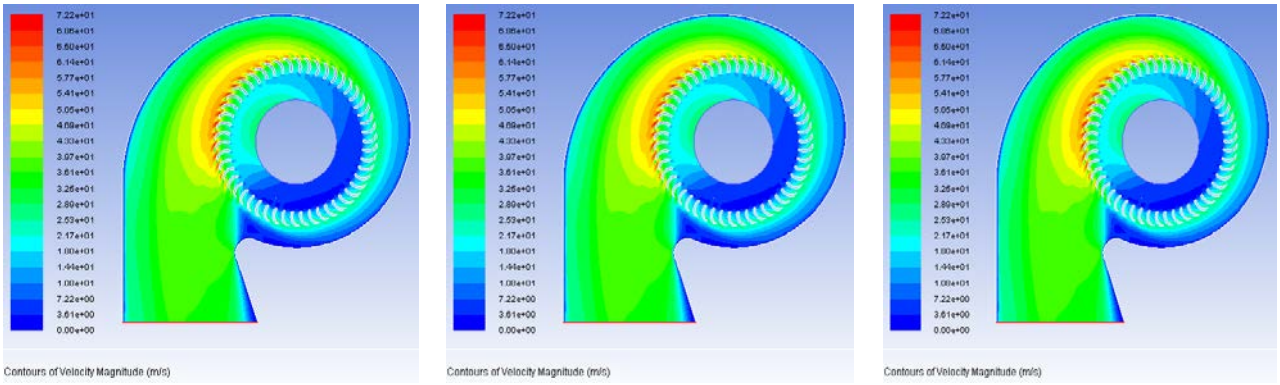
RESULTS AND DISCUSSIONS

The results of the numerical simulation of the centrifugal blower with forward-curved 30, 40 and 50 blades are presented with the pressure and velocity contours and velocity vector in Fig. 3, 4, and 5. From the Fig. 3, the minimum pressure occurs in the suctions of the impellers and it increases along volute casing however, the maximum pressure occurs approximately at the trailing edge of the blades.



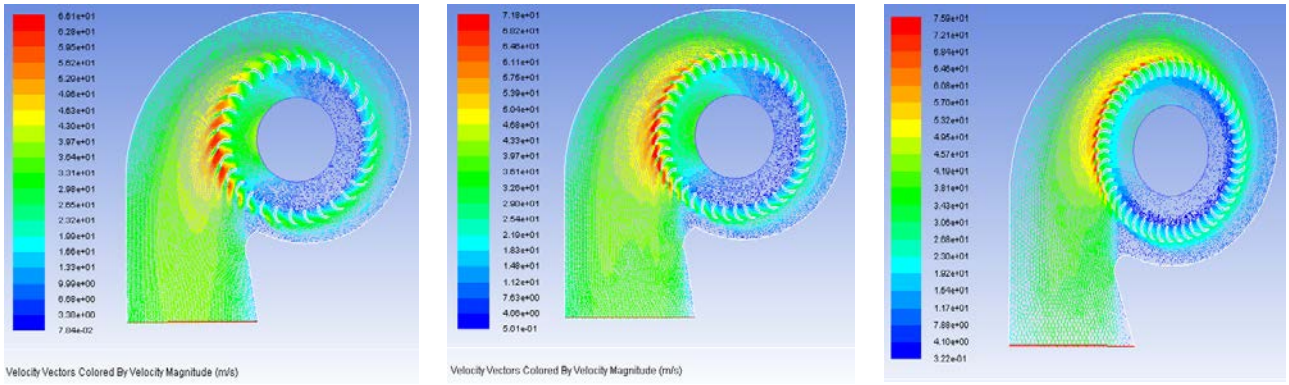
(a) 30 blades (b) 40 blades (c) 50 blades

Figure 3. The total pressure contours of the centrifugal blower with various blade numbers



(a) 30 blades (b) 40 blades (c) 50 blades

Figure 4. The velocity contours of the centrifugal blower with various blade numbers



(a) 30 blades (b) 40 blades (c) 50 blades

Figure 5. The velocity vectors of the centrifugal blower with various blade numbers

The velocity contours and vectors are presented in Fig. 4 and 5. The minimum velocity takes place on the volute casing wall due to no-slip boundary condition. The maximum velocity occurs approximately at the impeller blades trailing edge.

The total pressure and velocity magnitude at the outlet line are shown in Fig 3 and 4. From the Fig. 3, the total pressure at the outlet line increases with the increment in blade number. However it is clearly seen from Fig.4 that the velocity magnitude at the outline line decreases with the increase in the blade number.

From the Fig. 8, the shaft power of the blower increases while blade number increases from 30 to 50. On the other hand, the hydraulic efficiency of the blower decreases with the increment in blade number. Although hydraulic efficiency of the 30 and 40 blades close to each other, it decreases sharply from 40 to 50. The maximum efficiencies of the impellers are 59.90 % , 59.38 % and 48.32 % for the 30 blades, 40 blades and 50 blades, respectively.

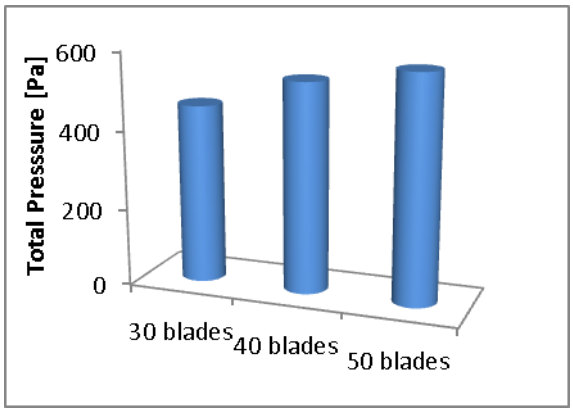


Figure 7. The area weighted average total pressures at the outlet line of the centrifugal blower with 30, 40 and 50 blades

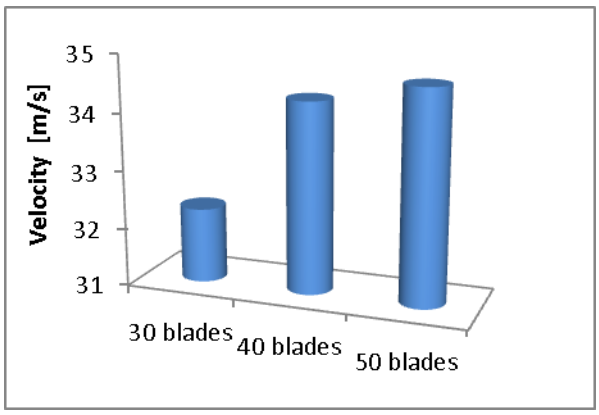


Figure 6. The area weighted average velocity magnitudes of the centrifugal blower with 30, 40 and 50 blades

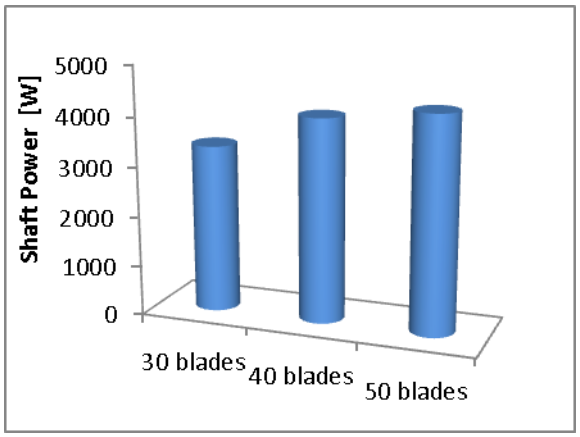


Figure 8. The shaft powers of the centrifugal blower with 30, 40 and 50 blades

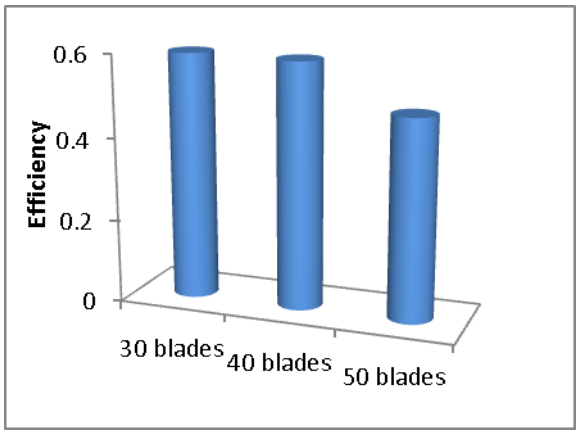


Figure 9. The hydraulic efficiencies of the centrifugal blower with 30, 40 and 50 blades

CONCLUSIONS

Recent developments in the Computational Fluid Dynamics (CFD) lead to specific important facilities to design turbomachines with the complex and the high turbulence internal flows. Thus, it allows interpreting the design procedure and optimizing the product components without the high cost and less waste of time before the manufacturing process. Besides, it enables us to study the effects of various parameters on these components.

The blade number is one of the most important parameter effect the centrifugal blower performance characteristics such as Head, Shaft Power and Efficiency.

The numerical results obtained in this study show that the increase in blade number from 30 to 50, cause to an increase at velocity magnitude and total pressure at the outlet line of the centrifugal blower additionally the shaft power of the centrifugal blower increases. However, the hydraulic efficiency of the centrifugal blower decreases with the increment in blade number.

REFERANCES

[1] M. S. CELLEK and T. ENGIN, 3-D numerical investigation and optimization of centrifugal slurry pump using computational fluid dynamics, J. of Thermal Science and Technology, 36, (1), 69-82, 2016.

[2] Fluent Inc., Tutorial 8. Using Multiple Rotating Reference Frames, January 11, 2005.

[3] Qi Datong, Mao Yijun, Liu Xiaoliang, Yuan Minjian, Experimental study on the noise reduction of an industrial forward-curved blades centrifugal fan, Applied Acoustics, 70, 1041–1050, 2009.

[4] Zhou W, Zhao Z, Lee TS, Winoto SH. Investigation of flow through centrifugal pump impellers using computational fluid dynamics. International Journal of Rotating Machinery; 9:49-61,2003.

[5] Madhwesh N, Karanth KV, Sharma NY, Member, IAENG. Impeller treatment of for a centrifugal fan using splitter vanes-A CFD Approach. Proceeding of the World Congress on Engineering, Vol. 3, London, U.K, 2011.

[6] Young-Tae Lee, Hee-Chang Lim, Performance assessment of various fan ribs inside a centrifugal blower, Energy, 94, 609-622, 2016.

[7] Beena D. Baloni, S.A. Channiwala, V.K., Mayavanshi., Pressure recovery and loss coefficient variations in the two different centrifugal blower volute designs. , 90, (1), 335-343, 2012.

[8] Qi Datong, Mao Yijun, Liu Xiaoliang, Yuan Minjian, Experimental study on the noise reduction of an industrial forward-curved blades centrifugal fan, Applied Acoustics, 70, 1041-1050, 2009.

[9] Singh RR, Nataraj M. Parametric study and optimization of centrifugal pump impeller by varying the design parameter using computational fluid dynamics: part I. Journal of Mechanical and Production Engineering (JMPE), 2: 87-97, 2012.

[10] Bacharoudis EC, Filios AE, Mentzos MD, Margaris DP. Parametric study of a centrifugal pump impeller by varying the outlet blade angle. The Open Mechanical Engineering Journal, 2:75-83, 2008.

[11] Singh RR, Nataraj M. Parametric study and optimization of centrifugal pump impeller by varying the design parameter using computational fluid dynamics: part I. Journal of Mechanical and Production Engineering (JMPE) 2012; 2:87-97.

[12] Versteeg HK, Malalasekera W. An introduction to computational fluid dynamics. (Longman Group Ltd, England)1998.

[13] Kyparissis SD, Douvi EC, Panagiotopoulos EE, Margaris DP, Filios AE. CFD flowfield analysis and hydrodynamic double-arc blade design effects for optimum centrifugal pump performance. International Review of Mechanical Engineering (I.RE.M.E.) 2009; 3:284-292.

[14] Engin T. Study of Tip Clearance Effects in Centrifugal Fans with Unshrouded Impellers Using Computational Fluid Dynamics. Proc. IMechE Part A: Journal of Power and Energy, 2006; 220:599-610.

Journal of Thermal Engineering

CONFERENCE ON ADVANCES IN MECHANICAL ENGINEERING ISTANBUL 2016 – ICAME2016
11-13 May 2016, Yildiz Technical University, Istanbul, Turkey

NUMERICAL INVESTIGATION ON JOURNAL BEARING LUBRICATION

*** MEHMET SALİH CELLEK**
Heat and Thermodynamics Division, Department of Mechanical Engineering, Mechanical Engineering Faculty, Yildiz Technical University, Yildiz, Besiktas, Istanbul 34349, Turkey

KAĞAN ÖZERK
Mechanical Engineer,
Consulting Sales Department Of Daikin, Istanbul, Turkey

AHMET DOĞAN
Heat and Thermodynamics Division, Department of Mechanical Engineering, Mechanical Engineering Faculty, Yildiz Technical University, Yildiz, Besiktas, Istanbul 34349, Turkey

ABDULKERIM OKBAZ
Heat and Thermodynamics Division, Department of Mechanical Engineering, Mechanical Engineering Faculty, Yildiz Technical University, Yildiz, Besiktas, Istanbul 34349, Turkey

İSMAIL ŞAHİN
Department of Machine Technology, Akyazi Vocational School, Sakarya University Akyazı/Sakarya/Turkey, 54400, Turkey

ALİ PINARBAŞI
Heat and Thermodynamics Division, Department of Mechanical Engineering, Mechanical Engineering Faculty, Yildiz Technical University, Yildiz, Besiktas, Istanbul 34349, Turkey

Keywords: Hydrodynamic Bearing, Lubrication, Grooved Journal
** Corresponding author: Phone:+900212 383 28 22*
E-mail address: mscellek@yildiz.edu.tr

ABSTRACT

In this study the bearing forces, which journal-bearing mechanisms carry, are examined in two different ways, theoretically and numerically. The numerical study is simulated with SolidWorks Flow Simulation. The numerical results obtained from the SolidWorks Flow Simulation show good agreement with the theoretical results.

Additionally, the effect of grooved shaft compared to the original (ungrooved shaft) is investigated at the same diameter, length, radial clearance and eccentricity. Finally, in order to increase the capability of bearing force, groove width and groove entrance angle are investigated.

INTRODUCTION

A bearing system function is to support an applied load by reducing friction between the relatively moving surfaces [1]. Journal bearing mechanisms, are extensively used in the piston engines, mainly transforms directional forces to the rotational forces.

The purpose of the mechanism is to form an oil film between shaft and bearing in order to decrease friction. If this essential condition is not occurred, the efficiency of shaft and bearing slides and mechanisms may effect negatively. Lack of oil film may also cause some other problems like high noise, high temperature and high bearing metal wear.

Protection of the mechanism for a long time is vital so that setting up of lubrication system must be well organized.

Shaft is located in lubricated bearing. The shaft rotates in the bearing and this rotation causes an oil film in the bearing. Thus the sliding begins without the metal to metal contact [2]. When the rotating velocity of the oil and viscosity increase, there is a space arises between shaft and bearing. Friction in the journal-bearing system decreases when this space increases. This is the main purpose of the study in the lubricated systems.

In the mechanism, high pressure occurs in the narrowing section and low pressure occurs in the expanding section. The bearing force is increases as an eccentricity ratio increases. Also, more pressure occurs in the middle

of the bearing relatively to the end sides of the bearing and the length of the bearing increases the bearing force increases.

The suitable journal bearing mechanism is chosen by considering the metal roughness and the planned force and likewise.

If metal roughness is too much, the mechanism needs more space between shaft and bearing for avoiding metal to metal contact. Therefore system needs to work with a low eccentricity ratio, so that system can carry less loads and this leads to demand bigger journal-bearing design.

The first analytical calculation based on Rayleigh step bearing model standard is presented by Wang et al. [3]. Nevertheless the equations for the infinite model he used are doubtful. It is concluded that for the cylindrical dimples there occurs a theoretical optimum of 40% in the dimple area ratio [4]. Quadoud et al.[5] studied thermohydrodynamic and thermoelastohydrodynamics of the journal bearing additionally they studied the thermo-elastic deformations of the solid parts. To determine the pressure, temperature and velocity distribution in the fluid film, finite volume method is used on the other hand the finite element method is used to determine the displacement field radial by using Computational Fluid Dynamics (CFD) and Fluid Structure Interaction (FSI). Additionally the effect of the rotational speed and eccentricity on the performance of the bearing investigated. It is stated that minimum film thickness is little affected by the elastic effects however the shape of the lubricant changes. On the other hand, Shenoy et al. [6] exhibited a methodology to model and simulate the Overall Elasto-Hyrodynamic Lubrication of of a full journal bearing utilized the sequential application of CFD and Computational Structural Dynamics (CSD). The pressure field for a full journal bearing operating under laminar flow regime with various L/D ratios is studied with CFD. Stress distribution and deformation in the bearing liner due to resulting pressure force is determined using FEM. From the result, it is expressed that ε has greater influence on the pressure than L/R ratios. It is stated in the studies of Quadoud et al.[5] and Shenoy et al.[6] that when complex geometries or detailed solutions are needed, general FSI codes make the analysis effective. Furthermore the FSI analysis is very convenient in the field of fluid film bearing analysis.

In this study, the bearing forces are investigated theoretically and numerically. Additionally, the effect of grooved shaft, groove width and groove entrance angle are investigated to increase the capability of the journal bearing.

THEORY

The bearing force is found with simulation and calculation when shaft is located in the bearing with 0, 5 eccentricity ratio. This means that minimum and maximum clearance between shaft and bearing are 0.125 mm. and 0.375 mm respectively.

The entrance of the shaft grooves is exposed low pressure if the clearance is more than the other sections resulting in oil enter the shaft.
At the part that oil film narrows and the middle parts of the shaft oil film changes their direction and this leads the oil discharge at front section. As a result high pressure happens at narrow part of and increases the carrying capacity considerably.

The depths of the grooves are taken 0,25 mm in every each simulation. Grooves enter 15mm in from beginning to the middle of the shaft with various angles according to shafts. The simulations have been done with the help of changing grooves entrance angle parameters and groove's width parameters.

Sommerfield Number has been found with the help of eccentricity ratio and l/d ratio as shown in the Figure 1.

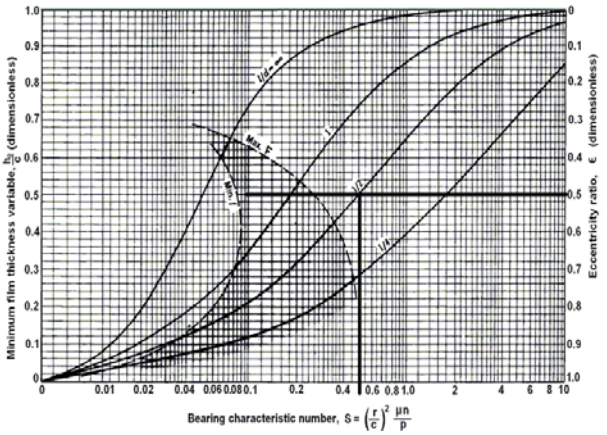


Figure 1. The finding of Sommerfield Number with the help of eccentricity ratio (0,5) and l/d ratio (1/2) [7]

Then Shaft's attitude angle has been found as 55,5° with the help of Sommerfield Number (0.5) and l/d ratio (1/2) shown in Figure 2.

Numerical investigation on journal bearing lubrication

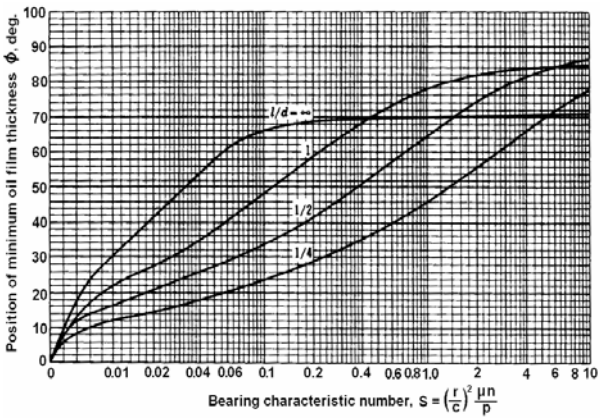


Figure 2. The finding of the shaft's attitude angle with the help of Sommerfield Number (0.5) and l/d ratio (1/2) [7]

Technical specifications of the bearing system are presented below.
Dynamic viscosity of the oil (μ): 1 Pa.s
Density of the oil (ρ): 892 kg/m^3
Angular Velocity (w): 97.67 rad/sec
Velocity: 0,58602 m/s
Eccentricity Ratio: 0.5
Length of shaft: 6mm
Diameter of the shaft 12 mm
Length of the shaft and bearing 6 mm
Bearing diameters 0.5 mm
Grooved depth: 0.25mm
The resultant force (W) is obtained with the W_x and W_y forces as follow

$W_y = ((\mu.U.L^3).\pi.\varepsilon)/(4.c^2.(1-\varepsilon^2)^{3/2})$ (5)
$W_x = ((\mu.U.L^3).\varepsilon^2)/(c^2.(1-\varepsilon^2)^{3/2})$ (6)
$W = (W_y^2 + W_x^2)^{1/2}$ (7)
Bearing force has been found by using formula 7.
W=1.519 N

MODEL AND SIMULATION OF UNGROOVED AND GROOVED JOURNAL BEARING

Journal bearing system has been modeled and then the mesh has been generated, in SolidWorks [8]. Lastly, the simulations have done with the SolidWorks Flow Simulation based on the above technical specifications. The CAD model of the journal bearing is shown in Figure 3.

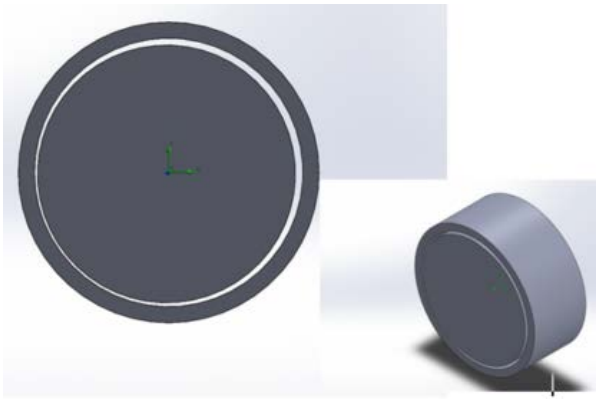


Figure 3: The model of the ungrooved Journal-Bearing mechanism.

The pressure distribution of the lubrication film is presented at Figure 4. From the figure it is clear that there are two pressure fields which are low and high.

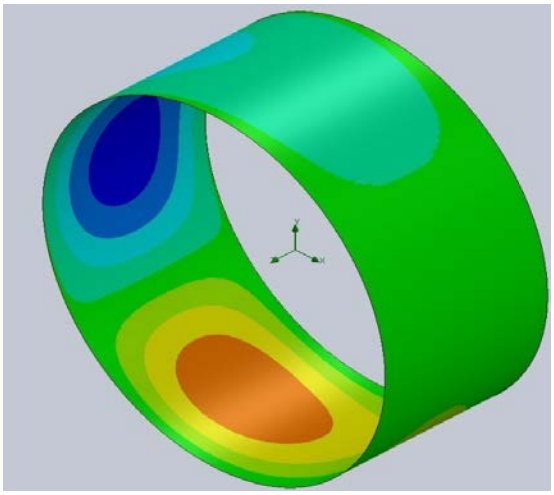


Figure 4**:** Pressure distribution of the ungrooved journal-bearing mechanism.

According to simulation result ungrooved shaft's bearing force is founded as W=1.465 N

The load capacity of ungrooved journal beairng mechanism is calculated and simulated. It can be seen from the theoritical and numerical results, the load capacity of both calculation are very close to each other as 1.597 N and 1.465 N.

Now, in order to increase carrying capacity of the journal bearing, the effects of the grooved journal bearing mechanism investigated. Then a parametric study is taken into account with the different grooved angle and width. The grooved journal bearing is shown in Figure 5.

Numerical investigation on journal bearing lubrication

The pressure distribution contours of the grooved journal bearing for three cases are illustrated in Figure 6-8. From the CFD simulation, the grooved journal bearing has been simulated with grooved angles from 25° to 65° and width from 0.5 to 2. When angle and width of the grooved journal bearing chosen 40° and 1.25 mm, the carring capacity increase to 1.874 N. From the Figure 7, as the angle and width chosen 25° and 0.5 mm, the carring capacity increases to 2.215 N. The load capacity of the all cases increase comparing with the ungrooved journal bearing. With the angle of 65° and the width of 1 mm, the carring capacity (W) reach to maximum at 2.462 N.

Moreover in order to investigate the effects of the grooved width and angle, different scenario has been performed and the results are graphed in Figure 9. At the angle of 30°, while the the journal groove width is 0.5 mm, journal bearing carries the highest load with the number of 2.215 N. At the angle of 65°, while the the journal groove width is 1 mm, journal bearing carries the maximum load with the number of 2.462 N. At the angle of 55°, while the the journal groove width is 1.25 mm, journal bearing carries the highest load with the number of 2.250 N. 1,5 mm witdh journal bearing cope with only 1.700 N. When the witdh of the model increase. At the low journal groove angles (25°-45°), the grooved journal loading capacity decreases with increase of groove width. On the other hand, the results are variable at the high angles. For instance, the journal bearing capacity is maximum with the grooved width of 1mm at angle of 65°. It is clear from the Figure 9 that,increasing the grove angles of journal from 45°to 65° the bearing capacity increases as well.

The comparison of the ungrooved and grooved journal bearing torque loss is shown in Figure 10 and 11. It is clear from the figures that the ungrooved torque loss is lower than the grooved one.

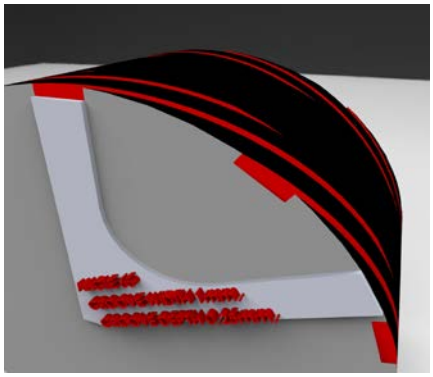


Figure 5**.** The model of groove journal bearing with the angle, width and depth are taken 65°, 1 mm and 0.25 mm

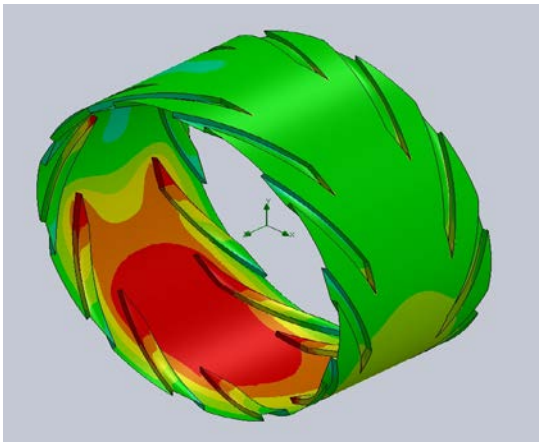


Figure 6**.** CFD analysis of the grooved journal bearing, the angle, width and depth are taken 40°, 1.25 mm. W= 1.874 N.

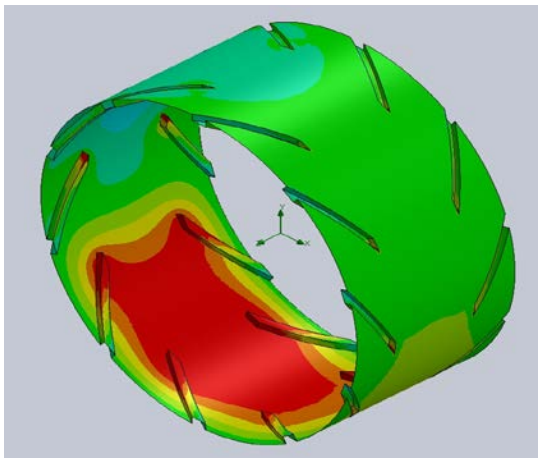


Figure 7**.** CFD analysis of the grooved journal bearing, the angle, width and depth are taken 25°, 0.5 mm, W= 2.215 N.

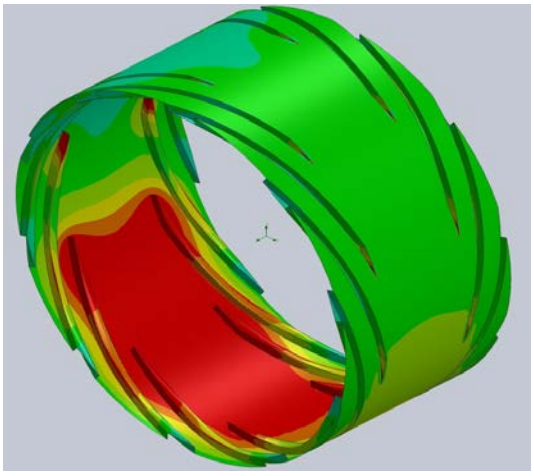


Figure 8**.** CFD analysis of the grooved journal bearing, the angle, width and depth are taken 65°, 1 mm.

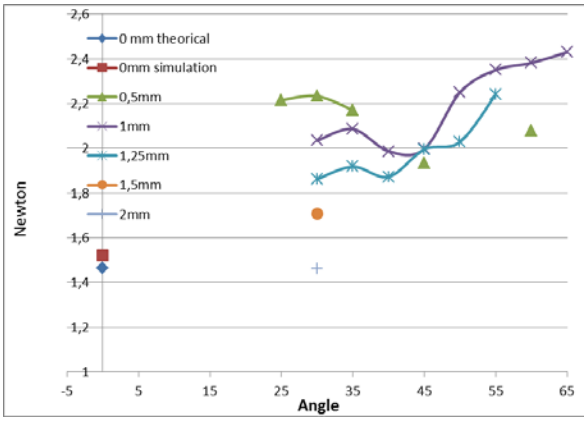


Figure 9**.** Each point in the table shows a bearing force which calculated or simulated by CFD analysis.

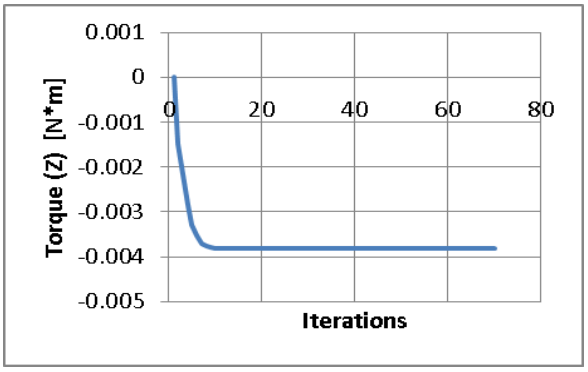


Figure 10**.** Ungrooved shaft torque loss
Mean of last 15 iterations: -0.003807773 N.m

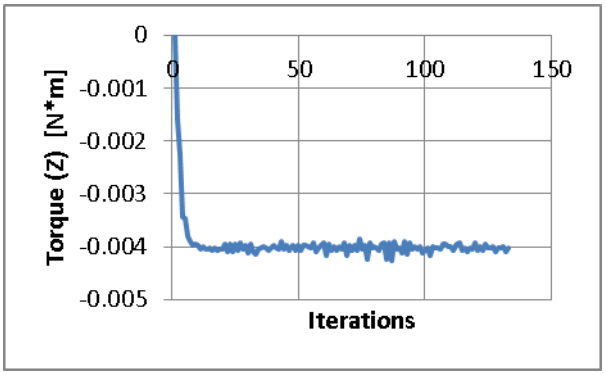


Figure 11. 1mm 65 deg, 10 grooved shaft torque loss

Mean of last 15 iterations: -0.00402669 N.m

CONCLUSION

Theoritical and numerical calculation of load capacity of the ungrooved journal beairng have been done. The results of both method are very close to each other.

Moreover, increasing carrying capacity of the journal bearing, the journal is grooved with various widths and angles. As a results of this, the carrying load capacity of journal bearing has increased significantly from 1,4653 N to 2,4626 N. In return, the disadvantages of the grooved journal leads to increase grooved shaft torque.

REFERANCES

[1] K.M. Pandey, P.L.Choudhury and N.P. Kumar., Numerical Unsteady Analysis of Thin Film Lubricated Journal Bearing, IACSIT Internationally Journal of Technology, vol. 4:2, 2012.

[2] C. Hervé, P.M.Perrier, and U.Baudis. "Nitrocarburizing: Arcor (R), a Controlled Ionic Liquid Process." *Encyclopedia of Tribology*. Springer US, 2013. 2428-2433.

[3] Wang, X., Kato, K., Adachi, K., Aizawa, K., Loads carrying capacity map for the surface
texture design of SiC thrust bearing sliding in water, Tribology International, Vol. 36, pp.
189-197, 2003.

[4] MARIAN, V.; PASCOVICI, M.; CICONE, Tr. Analytical and Numerical approach for load capacity of a single square cell from a textured surface. University" Politehnica" of Bucharest Scientific Bulletin, Series D: Mechanical Engineering, 2006, 68.3: 15-26.

[5] A.Quadoud, A. Mouchtachi, N. Boutammachte, Numerical simulation CFD, FSI of a hydrodynamic journal bearing, Journal of Advanced Research in Mechanical Engineering, 2, 33-38, 2011.

[6] S. B. Shenoy., R. S. Pai., D.S Rao., & R. B. Pai Elasto-hydrodynamic lubrication analysis of full 360'journal bearing using CFD and FSI techniques. World Journal of Modelling and Simulation, *5*(4), 315-320, 2009.

[7] A. Harnoy, Bearing Design in Machinery: Engineering Tribology and Lubrication, CRC Press, 2002.

[8] Dassault Systèmes SOLIDWORKS Corp.